Materials Research Express

Transfiguring structural, optical and dielectric properties of Cadmium thiourea acetate crystal by the addition of L-threonine for laser assisted device applications

To cite this article before publication: Rupali Balwant Kulkarni *et al* 2018 *Mater. Res. Express* in press https://doi.org/10.1088/2053-1591/aab2f8

Transfiguring structural, optical and dielectric properties of Cadmium thiourea acetate crystal by the addition of L-threonine for laser assisted device applications

Rupali B. Kulkarni[a,c], Mohd Anis[b], S. S. Hussaini[d] and Mahendra D. Shirsat*[,a]

[a] RUSA Centre for Advanced Sensor Technology, Department of Physics, Dr. Babasaheb Ambedkar Marathwada University, Aurangabad – 431004 (MS) INDIA

[b] Department of Physics, Sant Gadge Baba Amravati University, Amravati – 444602 (MS) INDIA

[c] Department of Physics, Swa. Sawarkar Mahavidyalaya, Beed 431122 (MS) INDIA

[d] Crystal Growth Laboratory, Department of Physics, Milliya Arts, Science & Management Science College, Beed-431122, Maharashtra, India.

* *Corresponding Author:* Tel.: +91 9422291987

E-mail address: mdshirsat.phy@bamu.ac.in

Highlights

- Premier report of the impact of LT on CTA crystal
- Enhanced transmittance of LT-CTA realized due to LT doping
- SHG efficiency of LT-CTA crystal 1.31(CTA) and shifted PL peak maxima is (517 nm)
- Z-scan revealed $\chi 3$ of order 4.81 x10-4esu and Figure of merit (FOM) 978.35
- Lower dielectric quality of LT-CTA crystal vital for optoelectronic applications

Abstract

Present investigation reports the growth of pure and L-threonine (LT) doped cadmium thiourea acetate (CTA) crystals by slow solution evaporation technique followed by structural, optical, thermal and dielectric characterization studies. A bulk single crystal of LT-CTA has been grown at temperature 38˚C. The single crystal X-ray diffraction technique has been employed to confirm the structural parameters of pure and LT doped CTA crystals. The increase in optical transparency of LT-CTA crystal was ascertained in the range of 200 to 900 nm using UV–visible spectral analysis. The widened optical band gap of the LT-CTA crystal is found to be 4.7 eV. Pure and doped crystals are subjected to FT-IR analysis to indicate the presence of functional groups quantitatively. Appreciable enhancement in second harmonic generation (SHG) efficiency of LT-CTA crystal with reference to parent CTA was confirmed from Kurtz–Perry SHG test (1.31 times of CTA crystal). The assertive influence of LT on electrical properties of grown crystals has been investigated in the temperature range 35-120˚C. Electronic purity and the color centered photoluminescence emission nature of pure and IA-CTA crystals were justified by luminescence analysis. With the aid of single beam *Z*-scan analysis, The Kerr lensing nonlinearity was identified and the magnitude of TONLO parameters has been determined. The cubic susceptibility ($\chi 3$) and Figure of merit (FOM) was found to be 4.81 $x10^{-4}$esu and 978.35. Results vitalize its application for laser stabilization systems.

Keywords: Crystal Growth, Dielectric studies, SHG efficiency, X-ray diffraction.

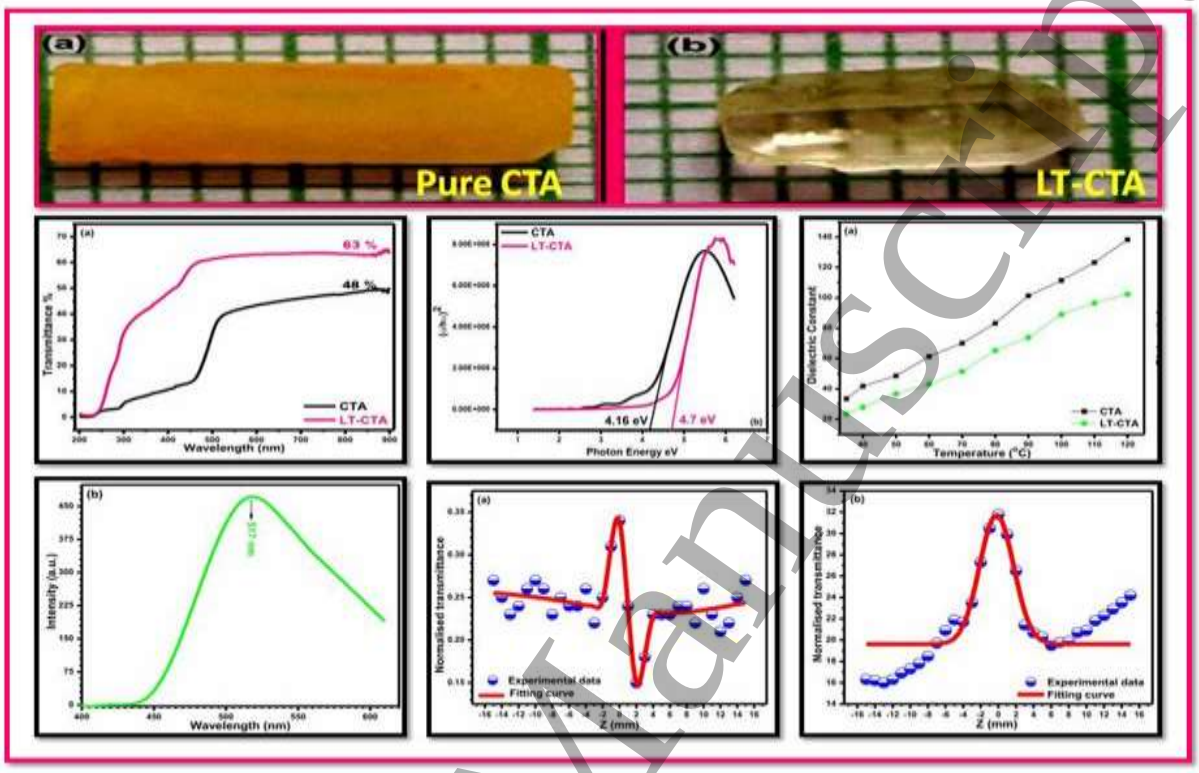

1. Introduction

Nonlinear optical (NLO) Thiourea metal complex (TMC) crystals have been very rapidly developed due to their appealing features such as large optical transparency, high nonlinear response, huge laser damage threshold, high thermal stability and improved mechanical rigidness. The presence of these qualities highlights TMC crystals liable for applications in electro-optic modulation, optical data storage devices, high-tech NLO and telecommunication devices [1-3]. The growth and study on characteristic properties of large number of TMC crystals such as BTZA, ZTC, BTCA, ZTS, CBTC, and BTCF have been reported [4-15], however cadmium thiourea acetate (CTA) outstands as an interesting NLO material with promising optical and physical performance. In order to achieve enhancement in properties of CTA crystal, doping of selected quantity of organic additive (in particular amino acid) play crucial role [16]. The amino acids are excellent organic additives to gain enhanced nonlinear optical response. The literature survey evidences that the doping of glycine, L-alanine has significantly enhanced the crystal perfection, optical transparency, second harmonic generation (SHG) efficiency, mechanical strength and dielectric properties of CTA crystal [17]. The constructive impact of L-cystine on structural, linear-nonlinear optical, laser damage threshold and surface properties of CTA crystal have been extensively studied [18]. The doping of L-valine has facilitated large improvement in dielectric, linear and third order nonlinear optical properties of CTA crystal [15].

The impressive and significant impact of amino acid on optical and electrical response of CTA crystal has attracted the attention of researchers in crystal growth field to investigate the characteristic features of CTA crystal by doping it with chiral amino acid, L-threonine (LT). LT is an exceptional amino acid which possesses high dipole moment as equal to water [19], wide –H bonding network and optically active chromospheres which are most prerequisite qualities vital for enhancing the optical, physical and dielectric performance of host crystal as evident in literature [20,21]. As per the literature survey, noteworthy fact is that till today no attempt has been made to explore the effect of chiral LT on transmutations of characteristic properties of CTA crystal. Therefore current study is aimed to analyze the structural, elemental, UV-visible; SHG efficiency and dielectric properties of LT doped CTA crystal using respective characterization techniques so as to improve the application of CTA.

2. Experimental procedure

The CTA complex has been synthesized by dissolving cadmium acetate (1mole) and thiourea (2mole) in double distilled de-ionized water. The CTA metal complex salt was repetitive recrystallized to gain highest possible purity for further synthesis. To achieve doping of LT, the supersaturated solution of purified CTA was prepared at room temperature. The measured quantity of 1wt% of LT was gradually added to the supersaturated solution of CTA with continuous stirring process to attain homogeneous doping throughout the mixture. The LT doped CTA solution was then filtered in a rinsed beaker and kept for slow solution evaporation in a constant temperature bath at 38 ^{0}C. The grown CTA and LT doped CTA (LT-CTA) single crystals are shown in Fig.1.

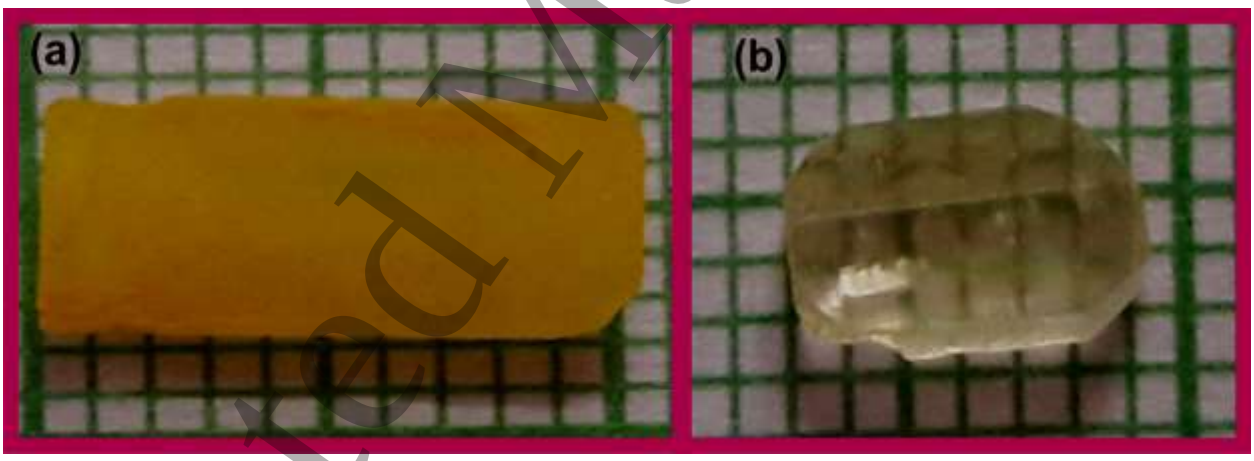

Fig.1 a) Pure CTA crystal b) LT-CTA crystal

3. Results and discussion

3.1 Single crystal X-ray diffraction (XRD) analysis

The single crystal XRD technique was employed using the Enraf Nonius CAD4 X-ray diffractometer to determine the structural parameters of grown pure and LT-CTA crystals. The XRD data shown in Table1 was recorded at room temperature and it confirmed the orthorhombic crystalline structure of pure and LT-CTA crystals. The analysis of XRD data evidences that the unit cell parameters of LT-CTA crystal show slight variation with reference to CTA and the large difference in cell volume infers the potential role of dopant LT in modifying the lattice dimensions of CTA crystal [20-21].

Table1. Single crystal XRD data

Crystal	a (A˚)	b (A˚)	c (A˚)	Volume $(A˚)^3$	Crystal system
CTA	7.57	11.79	15.41	1374	Orthorhombic
LT-CTA	7.59	11.83	15.47	1390	Orthorhombic

3.2 Fourier transforms infrared (FT-IR) analysis

The qualitative analysis of pure and LT-CTA crystal has been performed by means of FT-IR spectral analysis using the Bruker α-ATR spectrophotometer. The FT-IR spectrum of pure and LT-CTA crystal recorded in the range of 600-4000 cm^{-1} is plotted in Fig.2. The C-O-H bending vibration is attributed at 659 and 674 cm^{-1}. The C-S stretching vibration associated with thiourea of CTA is evident at 779 and 773 cm^{-1}. The peaks expressed at 1006 and 1011 cm^{-1} confirmed the =CH bond deformation. The C=S stretching vibration is observed at 1090 and 1099 cm^{-1}. The characteristic COO^- symmetric stretching associated with the CTA crystal is evident at 1396 and 1399 cm^{-1}. The major peaks of NO_2 antisymmetric stretching in grown crystals is contributed at 1538 and 1542 cm^{-1}.

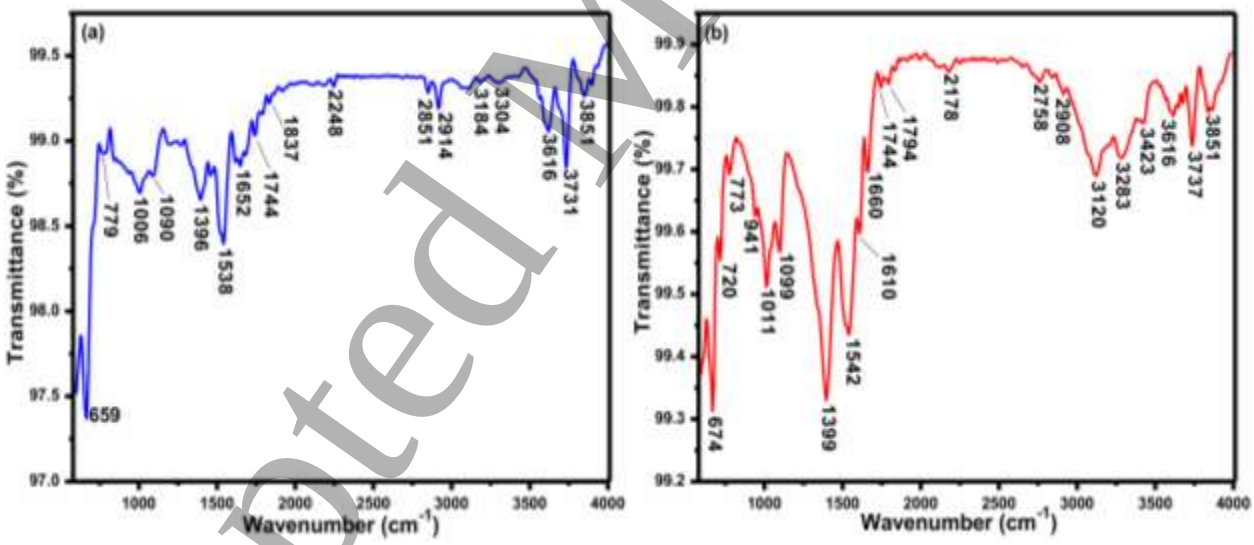

Fig.2 FTIR spectrum of (a) CTA (b) LT-CTA crystal.

The evidence of C=O bond stretching of carboxyl group is found at 1652, 1660, 1744, 1837 and 1794 cm^{-1}. The characteristic N=C=O antisymmetric stretching vibrations are attributed at 2248 and 2178 cm^{-1}. The antisymmetric stretching of NH_3^+ group is assigned at wavenumber 3184 and 3120 cm^{-1}. The peaks contributed with 3300-4000 cm^{-1} are contributed by NH and OH bond stretching vibrations. The vibration peaks are indexed in FT-IR spectrum and the observed shift in wavenumber of identified functional groups are distinguished in Table2.

Table2. FT-IR wave number assignments

Wavenumber (cm^{-1})	Functional group assignment

CTA	LT-CTA	
659	674	C-O-H bending
779	773	C-S stretching
1006	1011	=CH deformation
1090	1099	C=S stretching
1396	1399	COO^- symmetric stretching
1538	1542	NO_2 antisymmetric stretching
1652	1660	C=O stretching
1744	1744	C=O stretching
1837	1794	C=O stretching
2248	2178	N=C=O antisymmetric stretching
2851	2758	C-H stretching
2914	2908	C-H stretching
3184	3120	NH_3^+ antisymmetric stretching
3300-4000		NH and OH stretching

3.3 UV-visible study

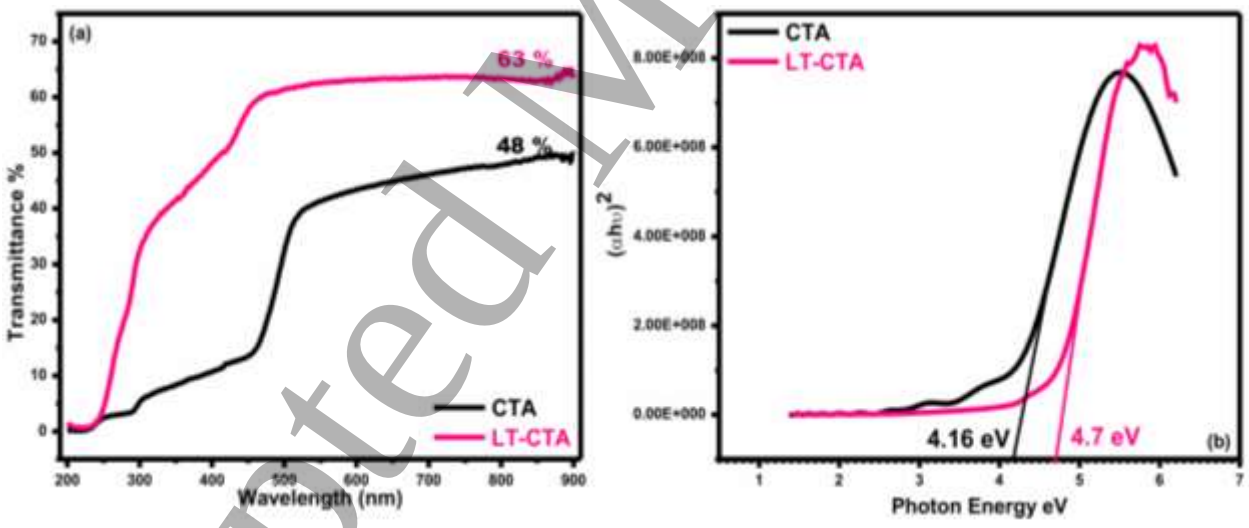

Fig. 3 (a) Transmittance spectrum (b) Tauc's plot

The electronic transitions associated with the functional chromospheres of crystal plays decisive role in facilitating the optical transmittance to designed crystal. The optically transparent crystals are readily demanded for photonics and NLO device applications [22-23]. In the present study, optical transmittance of 2 mm thickness pure and LT-CTA crystal has been ascertained in the wavelength range of 200 to 900 nm using the spectrophotometer (Shimadzu make UV-2450). The recorded transmittance spectrum is shown in Fig. 3a. The transmittance in a bulk crystal depends on two major factors (a) presence of optically active functional chromospheres and (b) the associated defect

centers and (c) crystal orientation [24]. The UV-visible spectrum of studied crystals confirm that the CTA crystal delivers the maximum transmittance of 48% and the LT-CTA crystal exhibits the enhanced transmittance up to 63% in entire visible region. The cutoff wavelength of grown crystals is found to be 230 nm. The optical transmittance of LT-CTA crystal is found to be 15% higher as compared to CTA crystal which might have been expressed due to less optical scattering and absorption of light in crystal medium [18]. The collective effect of high transmittance tendency of amino acid (LT in present case) [25] and minimized structural and crystalline defects [14, 26] might have favored the observed enhancement in %transmittance of LT-CTA crystal. The LT-CTA crystal with high optical transmittance can be advantageous for UV-tunable lasers and NLO device applications [03]. The optical band gap of LT-CTA crystal has been calculated using the Tauc's plot (Fig. 3b) drawn using equation, $(\alpha h\nu)^2 = A(h\nu - E_g)$ [27]. The optical band gap of LT-CTA crystal is found to be 4.7 eV, which is comparatively larger than the band gap of glycine doped CTA crystal (3.55 eV) [16]. The presence of amine group facilitates significant enhancement in band gap of host crystal [28] which is also observed in LT-CTA crystal. The high band gap value indicates that LT-CTA crystal has wide optical transmission rage and suggests its potential candidature for optoelectronics device applications [29].

3.4 SHG efficiency test

The NLO behaviour i.e. frequency conversion efficiency has been determined using the powder technique developed by Kurtz and Perry [30]. In the present analysis, the Q-switched mode operated Nd: YAG laser (1064 nm, 10 Hz, 8 ns, 680 mW) has been used to determine the SHG efficiency of studied crystals. A fine powder of optical quality pure and LT-CTA crystals was prepared and tightly sieved in a micro-capillary tube of uniform bore. The Gaussian filtered beam of Nd: YAG laser was multi-shot on the prepared samples and the generated output signal was collected through the array of the photomultiplier tube. The emergence of bright green light from the sample confirmed the NLO behaviour in grown crystals. The optical signals of the respective samples were simultaneously converted into energy using the digital power meter. The output energy for CTA and LT-CTA crystal sample was found to be 1.6 mJ and 2.1 mJ respectively (Table3). The prominent charge transfer between dopant and host crystal matrix might have contributed significant enhancement in SHG efficiency of LT-CTA crystal which is found to be 1.31 times higher than CTA crystal material. The enhanced SHG efficiency indicates the prime suitability of LT-CTA crystal for frequency conversion and optical modulation device applications [31].

Table.3. SHG efficiency data

Crystal	Output Voltage	SHG efficiency	
		Reference KDP	Reference CTA
KDP	1.35	1	0.84
CTA	1.6	1.18	1
CTA+LT (0.25 wt%)	1.8	1.33	1.12
CTA+LT (0.5 wt%)	1.93	1.42	1.2
CTA+LT (1 wt%)	2.1	1.55	1.31

3.5 Dielectric studies

The dielectric constant and dielectric loss of pure and LT-CTA crystal have been examined in the temperature range of 35-120˚C using the LCR tester (HIOKI 3532). For accurate data measurement, the crystal samples were applied by the silver paste to attain good electrical contact and subjected to dielectric analysis. For studied crystals, the variation of dielectric constant with temperature ($\varepsilon r = Cd/\varepsilon 0A$) is depicted in Fig.4a.

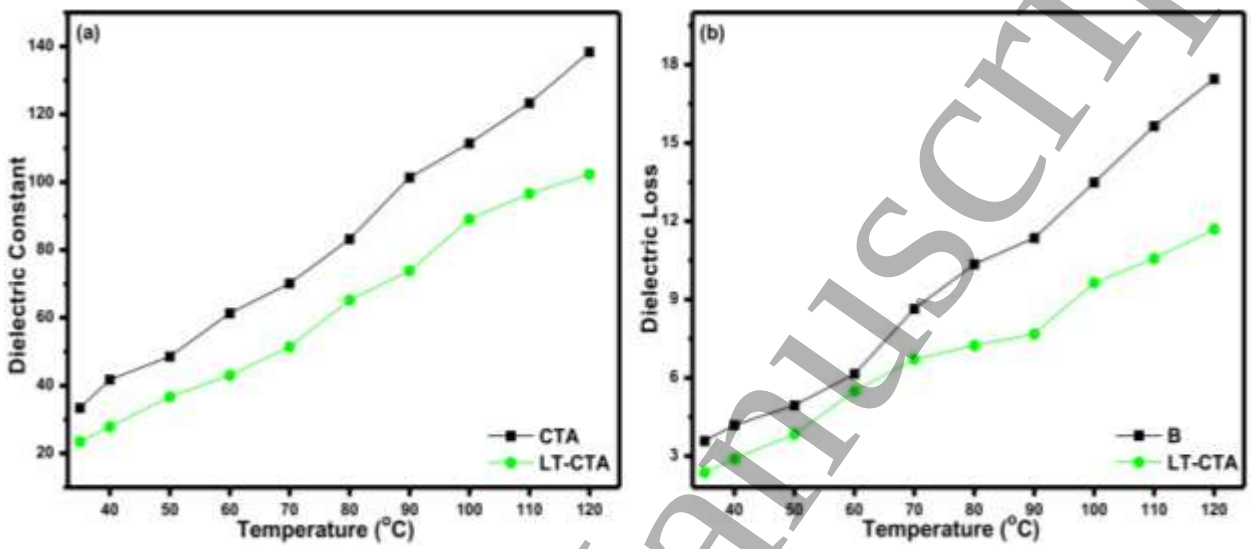

Fig.4 Temperature dependent (a) dielectric constant (b) dielectric loss

The relaxation tendency of molecular dipoles and the electronic, ionic, dipolar and space charge polarization activity associated with the material are the key factors responsible for the origin of dielectric constant [13]. At higher temperatures, the dielectric constant is majorly attributed to the dominance of space charge polarization [32] hence the dielectric constant of pure and LT-CTA crystal increases with increase in temperature as shown in Fig.4a. The lower dielectric constant of LT-CTA crystal accredited the low electrical power consumption capability [47]. Miller's law states that the lower dielectric constant facilitates the enhancement in SHG coefficient of the crystal [47], validated by LT-CTA crystal.

The dielectric loss profile of grown crystals is shown in Fig.4b which evaluates the extent of loss of electrical energy in the form of heat in material medium [47]. It reveals that the dielectric loss of crystals increases with increase in temperature. The analysis of dielectric loss gives the information regarding loss of energy through intrinsic and extrinsic defects present in crystal medium [33-35]. The lower dielectric loss in LT-CTA crystal suggests the presence of minimum electrically active defects [36].

It is noteworthy that the dielectric constant and dielectric loss of LT-CTA crystal is lower as compared to CTA. Thus, LT-CTA crystal is found to be more promising material than CTA for designing microelectronics, THz wave generators, photonics, broadband electro-optic modulators, field detectors and optoelectronics devices [37-38].

3.6 Photoluminescence studies

The comparison of photoluminescence (PL) spectrum of material for identification of modifications or external impurities in standard compounds is largely practiced technique in biomedical and chemical industries. The PL spectrum gives essential information regarding the electronic impurities and electronic transitions associated with the concerned material [39]. In the present analysis, the pure and LT-CTA crystal materials were photo-excited with

the high emission wavelength of 354 nm and 320 nm respectively and the PL spectrum was recorded in the range of 400 to 600 nm. The recorded PL emission spectrum of pure and LT-CTA crystal material is shown in Fig. 5a and 5b respectively. The CTA crystal material exhibits the blue colour emission whose peak maxima is centered at 481 nm whereas the LT-CTA crystal material exhibits the green colour emission with peak maxima centered at 517 nm. In addition to enhancement in PL intensity, the doping of LT resulted to shift in wavelength of emission peak maxima of CTA crystal which is ideal characteristic for impurity detection. The decrease in PL intensity in higher wavelength region might have been occurred due to less rotation of proton populated carboxyl group surrounded by central C–C bond associated with pure and LT-CTA crystal materials [03, 40]. The change in photoluminescence nature of CTA crystal due to the addition of LT might be advantageous for biomedical and biochemical device applications for antibody detection or manifesting external element [41-42].

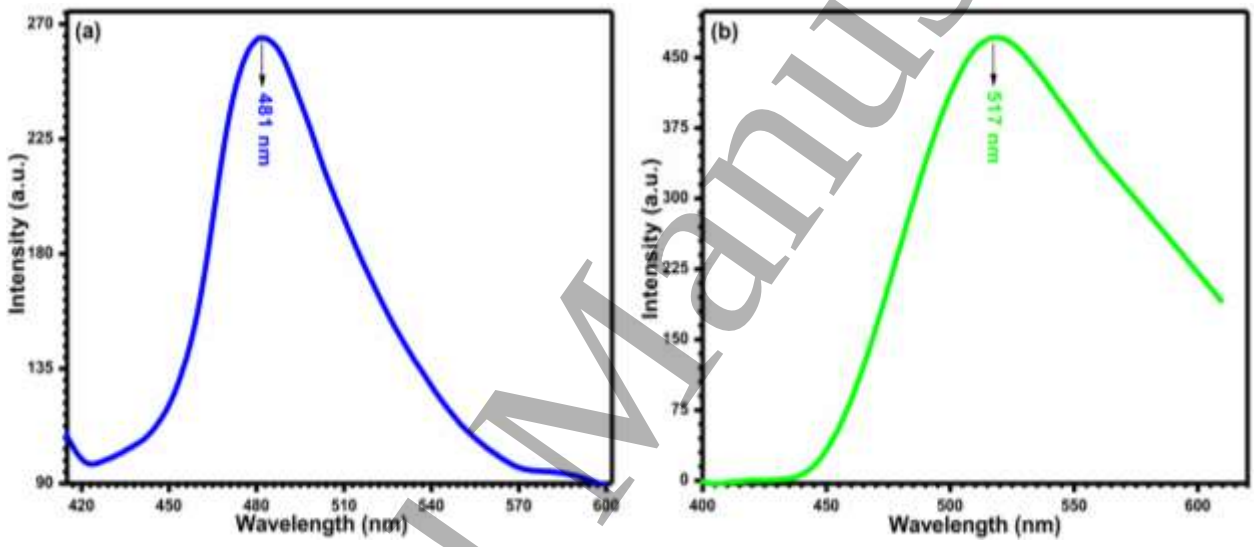

Fig.5 PL emission spectrum of (a) CTA (b) LT-CTA

3.7 Z-scan Analysis.

The third order nonlinear response attributed by pure and LT-CTA crystal at 632.8 nm has been investigated by means of He-Ne laser assisted Z-scan technique developed by Bahae et al.[43]. The resolution of Z-scan setup is detailed in Table4. The simultaneous measurement was carried using open and closed aperture data to examine the nature of nonlinear index of refraction (n_2) and nonlinear absorption coefficient (β). The nonlinear refraction phenomenon can be understood with the analysis of closed aperture intensity dependence of the crystal along pre and post the focus point [44]. A Gaussian beam is focused by a spherical lens onto the sample using a lens of focal length 30mm placed at a far field. The variation in intensity due to the displacement of a sample along the Z direction is monitored through a small aperture placed at the field point. The behavior of nonlinear absorption coefficient is of vital importance which can be illustrated on the basis of open aperture transmittance data of title material. The difference between the peak and valley transmission (ΔTp-v) is written in terms of the on-axis phase shift at the focus as,

$$\Delta T_{p-v} = 0.406(1-S)^{0.25}\left|\Delta\phi\right| \quad (5)$$

Where, S is the aperture linear transmittance, $S = 1 - \exp(-2r_a^2 / \omega_a^2)$ (6)

Where, r_a is the aperture and ω_a is the beam radius at the aperture. The nonlinear refractive index is given by,

$$n_2 = \frac{\Delta\phi}{KI_0L_{eff}} \quad (7)$$

Where, $K = 2\pi / \lambda$ (λ is the laser wavelength), I_0 is the intensity of the laser beam at the focus (Z=0), $L_{eff} = [1- \exp(-\alpha L)]/ \alpha$ is the effective thickness of the sample, α is the linear absorption and L is the thickness of the sample. From the open aperture Z-scan data, the nonlinear absorption coefficient is estimated as, $\beta = \frac{2\sqrt{2}\Delta T}{I_0 L_{eff}}$ (8)

Where, ΔT is the one valley value at the open aperture Z-scan curve. The value of β will be negative for saturable absorption and positive for reverse saturable absorption (RSA). The third-order nonlinear optical susceptibility $\chi(3)$ in its real and imaginary parts is defined as follows,

$$\mathrm{Re}\,\chi^{(3)}(esu) = 10^{-4}(\varepsilon_0 C^2 n_0^2 n_2) / \pi(cm^2 / W) \quad (9)$$

$$\mathrm{Im}\,\chi^{(3)}(esu) = 10^{-2}(\varepsilon_0 C^2 n_0^2 \lambda\beta) / 4\pi^2(cm / W) \quad (10)$$

Where, ε_0 is the vacuum permittivity, n_0 is the linear refractive index of the sample and c is the velocity of light in vacuum. Thus, we can easily obtain the absolute value of χ^3 using equation,

$$\chi^3 = \sqrt{(\mathrm{Re}\,\chi^3)^2 + (\mathrm{Im}\,\chi^3)^2} \quad \text{esu} \quad [45] \quad (11)$$

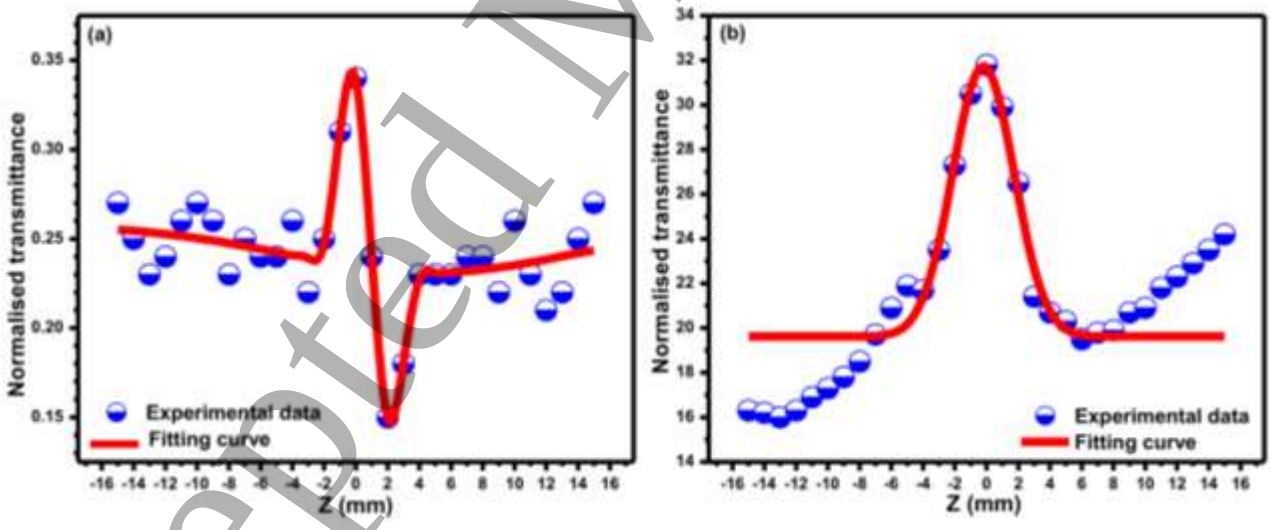

Fig.6 (a) closed aperture Z-Scan curve (b) Open aperture Z-Scan curve

Table4. Optical resolution of the Z-scan setup

Parameters and Notations	Details
Laser beam wavelength (He-Ne) (λ)	632.8nm
Lens focal length (f)	30mm
Optical path length(Z)	85 cm

Beam radius of the aperture (w_a)	3.3mm
Aperture radius(ra) for closed aperture	2 mm
Incident intensity at the focus	26.5MW/cm^2)

The closed aperture transmittance data depicted in Fig.6a confirms the self-defocusing nature as pre-focal transmittance peak is followed by the post-focal transmittance valley indicating the negative index of refraction which suggests its prominence for the protection of optical night vision sensor devices [46]. The shifts observed in maximum valley transmittance of close and open aperture curves of LT-CTA crystal (Fig.6a and 7b) confirm that LT is the potential dopant to tailor TONLO properties of CTA crystal.

The nonlinear refractive (NLR) index is found to be – 4.45 x10^{-12}cm/W. NLR relates directly to the prominent Kerr-lens mode locking (KLM) ability of the crystal. The High magnitude of NLR (10^{-12}) suggests the strong Kerr-lensing effect [47-48] which advocates the prominence of LT-CTA crystals for analyzing the stability limits of continuous-wave mode-locked laser systems and generating the shorter laser pulses.

The TONLO absorption coefficient β is the measurable parameter from the open aperture Z-scan configuration. The traced open aperture Z-scan transmittance curves have been analyzed to unearth the TONLO absorption tendency of pure and LT-CTA crystal. Open aperture transmittance curve (Fig.6b) reveals that as the sample is translated along Z-direction, the intensity of transmittance increases at the focus confirming the existence of saturable absorption (SA) phenomenon in LT-CTA crystal. The origin of SA effect is facilitated by the dominance of ground state linear absorption coefficient over the excited state absorption [30]. The effective β value of LT-CTA crystal is found to be 6.88 x x10^{-5}cm/W calculated by using equation (8).

The nonlinear third order susceptibility of LT-CTA crystal is found to be 4.81 x 10^{-4}esu which is notably greater than efficient third-order NLO crystals [02, 15]. LC-CTA crystal has a high magnitude of $\chi 3$ (10^{-4}esu) which might have been facilitated by photo-induced π-electron delocalization along large bonding network developing the strong polarizing potential in crystal [18]. In the regime of TMC crystals, the third order nonlinear susceptibility of LT-CTA crystal is found remarkably higher than L-Cysteine and L-Valine doped CTA crystals[18-19], thiourea, BTZB, ZTS, BTZC and BTCF crystals [02,15,49].

The figure of merit (FOM=β $\lambda/n_2$is a decisive parameter to ascertain the worthiness of crystal for optical power limiting applications [19]. The FOM value for LT-CTA crystal is found to be 978.35 which suggest its potential candidature for optical power limiting applications. Also, the FOM value is appreciably larger than L-Cysteine and L-Valine doped CTA crystals [15, 18].The LT-CTA crystal with attractive nonlinear properties (Table5) holds the huge advantage for optical switching, optical logic gates, calibrating optical distortions, passive laser mode-locking systems and also suggests its suitability for applications in laser stabilization, optical limiting and sensor devices [50-52].

Table5. TONLO parameters

Sample	n_2 (cm^2/W)	β (cm/W)	$\chi 3$ (esu)	FOM	Reference
Pure CTA	8.37 x10^{-11}	4.70 x10^{-6}	2.58 x10^{-4}	35.57	[18]
LC-CTA	4.85 x10^{-12}	1.19 x10^{-5}	6.18 x10^{-5}	156	[18]

LV-CTA	5.06 $x10^{-11}$	9.05 $x10^{-6}$	3.34 $x10^{-4}$	113.1	[15]
LT-CTA	**4.45 $x10^{-12}$**	**6.88 $x10^{-5}$**	**4.81 $x10^{-4}$**	**978.35**	**[present work]**

4. Conclusions

Single crystals of pure and LT-CTA material have been grown by slow solution evaporation technique. In UV-visible studies the LT-CTA crystal is found optically transparent up to be 63%. The vibration peaks are indexed in FT-IR spectrum and the observed shift in wave number of identified functional groups confirmed the doping of LT in CTA. The SHG efficiency of LT-CTA crystal is found to be 1.31 times higher than CTA crystal which is vital for NLO applications. In studied temperature range, the LT-CTA crystal attributed lower dielectric constant and dielectric loss as compared to CTA crystal. The doping of LT changed the photoluminescence tendency of CTA crystal from blue (481 nm) to green (517 nm) color which is promising quality for detection applications. In close aperture Z-scan analysis negative refraction nonlinearity has been attributed by LT-CTA crystal. The magnitude of n_2, β and $\chi 3$ is 4.45 $x10^{-12}cm^2/W$, 6.88 $x10^{-5}$ cm/W and 4.81 $x10^{-4}$esu for LT-CTA crystal. The open aperture Z-scan analysis revealed the saturable absorption effect in crystal with LT-CTA crystal. It is worth mentioning that the LT offered switching in TONLO behavior of CTA crystal. Hence LT-CTA crystal holds strong status for applications in the holographic data storage, frequency convertors, solar coating, optical switching devices, night vision sensors, electro-optic modulators and THz wave generator included under the extended umbrella of photonic device applications.

Acknowledgments

Authors are grateful to UGC-SAP, New Delhi, India (F.530/16/DRS-I/2016 (SAP-II)), Director, RUSA Centre for Advanced Sensor Technology, Dr. Babasaheb Ambedkar Marathwada University Aurangabad, India for providing technical support, also thanks to Prof. Kalainathan (Crystal Growth center, VIT Vellore, India) and Dr. M.S. Pandian (S.S.N. College of Engineering, Chennai, India) for extending Z-scan and the photoluminescence facility. Author Mohd Anis is thankful to UGC, New Delhi, India for awarding the Maulana Azad National Fellowship **(**F1-17.1/2015-16/MANF-2015-17-MAH-68193).

References

[1] R. Uthrakumar, C. Vesta, C. Justin Raj, S. Krishnan, S. Jerome Das, Curr. Appl. Phys.10 (2010) 548-552.

[2] N. N. Shejwal, Mohd Anis, S. S. Hussaini, M. D. Shirsat, Phys. Scr. 89 (2014) 125804-125810.

[3] Mohd Anis, S. S. Hussaini, M.D. Shirsat, Optik 127 (2016) 9734-9737.

[4] G. Pabitha, R. Dhanasekaran, Opt. Laser Technol. 50 (2013) 150-154.

[5] Mohd Anis, R. N. Shaikh, M. D. Shirsat, S. S. Hussaini, Opt. Laser Technol. 60 (2014) 124-129.

[6] R. Sankar, C. M. Raghavan, R. Jayavel, Cryst. Res. Technol. 41(2006)919–924.

[7] S. Shahil Kirupavathy, S. Stella Mary, P. Srinivasan N. Vijayan, G. Bhagavannarayana, R. Gopalakrishnan, J. Cryst. Growth 306(2007)102–110.

[8] J. Uma and V. Rajendran, Ind. J. Comp. Appl. 30 (2011)8–10.

[9] K. Kanagasabapathy, R. Rajasekaran, Optoelec. And Adv. Mat. – Rapid Comm. 6(2012) 218 – 224.

[10] M. Anis, S.S. Hussaini, A. Hakeem, M.D. Shirsat, G.G. Muley, Optik-International Journal for Light and Electron Optics 127(2016)2137-2142.

[11] M. Anis, G.G. Muley, M.D. Shirsat, S.S. Hussaini, Materials Research Innovations 19 (2015)338-344.

[12] V.G. Pahurkar, Mohd Anis, M.I. Baig, S.P. Ramteke, B. Babu, G.G. Muley, Optik 142 (2017) 421-425

[13] S.M. Azhar, M. Anis, S.S. Hussaini, M.D. Shirsat, G. Rabbani, Optik-International Journal for Light and Electron Optics 127 (2016) 4932-4936.

[14] N.N. Shejwal, M. Anis, S.S. Hussaini, M.D. Shirsat, Optik-International Journal for Light and Electron Optics 127 (2016), 6525-6531.

[15] M. Anis, S.S. Hussaini, M.D. Shirsat, G.G. Muley, Materials Research Innovations 20 (2016)312-316.

[16] S.S. Kirupavathy, S.S. Mary, P. Mythili, R. Gopalakrishnan, J. Cryst. Growth 310 (2008) 2555-2562.

[17] V. Ganesh, T. Bhaskar Rao, K. Kishan Rao, G. Bhagavannarayana, Mohd. Shkir, Mater. Chem. Phys. 137 (2012) 276-281.

[18] S.M. Azhar, Mohd Anis, S.S. Hussaini, S. Kalainathan, M.D. Shirsat, G. Rabbani, Opt. Laser Technol. 87 (2017) 11-16

[19] D. Jaikumar, S. Kalainathan, Cryst. Res. Technol. 43 (2008) 565-571.

[20] Mohd. Shakir, V. Ganesh, B. Riscob, K.K. Maurya, K. Kishan Rao, M.A. Wahab, G. Bhagavannarayana, Int. J. Pure Appl. Phys.7 (2011) 13-24.

[21] Mohd. Shkir, V. Ganesh, S. AlFaify, H. Algarni, G. Bhagavannarayana, K.K. Maurya, M.M. Abutalib, I.S. Yahia, Mater. Res. Innov. 21 (2017) 106-114.

[22] R. Subhashini, D. Sathya, V. Sivashankar, P.S.L. Mageshwari, S. Arjunan, Opt. Mater. 62 (2016) 357-385.

[23] M. Saravanan, Opt. Mater. 58 (2016) 327-341.

[24] M.I. Baig, Mohd Anis, G.G. Muley, Optik 131 (2017) 165-170.

[25] M.S. Pandian, P. Ramasamy, J. Cryst. Growth 312 (2010) 413-419.

[26] M.S. Pandian, P. Ramasamy, Binay Kumar, Mater. Res. Bull. 47 (2012) 1587-1597.

[27] Mohd Anis, M.S. Pandian, M.I. Baig, P. Ramasamy, G.G. Muley ,Mater. Res. Innov. (2017) https://doi.org/10.1080/14328917.2017.1329992

[28] Bhuvana K. Periyasamy, Robinson S. Jebas, N. Gopalakrishnan, T. Balasubramanian, Mater. Lett. 61 (2007) 4246-4249

[29] Mohd Anis, S.P. Ramteke, M.D. Shirsat, G.G. Muley, M.I. Baig, Opt. Mater. 72 (2017) 590-595

[30] S.K. Kurtz, T.T. Perry, J. Appl. Phys. 39 (1968) 3698-3813.

[31] Mohd Anis, M.D. Shirsat, Gajanan Muley, S.S. Hussaini, Phys. B 449 (2014) 61-66.

[32] Mohd Anis, G.G. Muley, Phys. Scr. 91 (2016) 85801-85808.

[33] Mohd Anis, D.A. Hakeem, G.G. Muley, Results Phys. 6 (2016) 645-650.

[34] Min-hua Jiang, Qi Fang, Adv. Mater. 11 (1999) 1147-1151.

[35] N. Bhuvaneswari, K. Baskar, R. Dhanasekaran, Optik 126 (2015) 3731-3736.

[36] Mohd Anis, G.G. Muley, V.G. Pahurkar, M.I. Baig, S.R. Dagdale, Mater. Res. Innov. 22 (2018) 99-106

[37] Mohd Anis, G.G. Muley, M.I. Baig, S.S. Hussaini, G.G. Muley Mater. Res. Innov. 21 (2017) 439-446

[38] Mohd Anis, S.S. Hussaini, Mohd Shkir, S. Alfaify, M.I. Baig, G.G. Muley Optik 157 (2018) 592-596

[39] Timothy H. Gfroerer, Encyclopedia of Analytical Chemistry, (2000) 9209-9231.

[40]A. Aravindan, R. Gopalakrishnan, P. Ramasamy Cryst. Res. Technol. 42 (2007) 1097-1103.

[41] S.P. Ramteke, Mohd Anis, M.I. Baig, Mohd Shkir, V. Ganesh, G.G. Muley Optik 158 (2018) 634-638

[42] S.P. Ramteke, Mohd Anis, M.I. Baig, G.G. Muley 154 (2018) 275-279

[43]Sheik-Bahae MS, Said AA, Wei T-H, IEEE J Quant Electron. 26(1990)760-769.

[44]S. Dhanuskodi, A. Philominal, J. Philip, K. Kim, J. Yi, J. Mater. Sci. 46 (2011) 3169-3175.

[45]J. Wen, Ch. Y. Gao, H. T. Yu, M. Zhao, J. J. Shang, Applied Physics B, 123 (2017) 85.

[46]P.V. Dhanaraj, N.P. Rajesh, J. Cryst.Growth 318 (2011) 974-978.

[47]Mohd Anis, M.D. Shirsat, S.S. Hussaini, B. Joshi, G.G. Muley, J. of Mat. Sci. & Tech. 32 (2016) 62–67.

[48]Y.B. Rasal, Mohd Anis, M. D. Shirsat, S. S. Hussaini, Materials Research Innovations, (2017) http://dx.doi.org/10.1080/14328917.2017.1327199

[49]T.C.SabariGirisun, S.Dhanuskodi, D.Mangalaraj, J.Phillip, Curr.Appl.Phys.11 (2011)838–843.

[50] R.N. Shaikh, Mohd Anis, M.D. Shirsat, S.S.Hussaini Optik 154 (2018) 435-440

[51]P.T. Anusha, P. Silviya Reeta, L. Giribabu, S.P. Tewari, S. Venugopal Rao, Mater. Lett.64 (2010) 1915-1917.

[52] S.P. Ramteke, Mohd Anis, M.S. Pandian, S. Kalainathan, M.I. Baig, P. Ramasamy, G.G. Muley Opt. Laser Technol. 99 (2018) 197-202

Figure Captions

Fig.1 a) Pure CTA crystal b) LT-CTA crystal

Fig.2 FTIR spectrum of (a) CTA (b) LT-CTA crystal.

Fig.3 (a) Transmittance spectrum (b) Tauc's plot

Fig.4 Temperature dependent (a) dielectric constant (b) dielectric loss.

Fig.5 PL emission spectrum of (a) CTA (b) LT-CTA

Fig.6 (a) closed aperture Z-Scan curve (b) Open aperture Z-Scan curve